

Study of flavour dependencies in leptogenesis

F. X. Josse-Michaux, A. Abada

*Laboratoire de Physique Théorique, UMR 8627, Université de Paris-Sud 11, Bâtiment 210,
91405 Orsay Cedex, France*

Abstract

We study the impact of flavours on the efficiency factors and give analytical and numerical results of the baryon asymmetry taking into account the different charged lepton Yukawa contributions and the complete (diagonal and off-diagonal) L to $B - L$ conversion A matrix. With this treatment we update the lower bound on the lightest right-handed neutrino mass.

1 Introduction

The minimal leptogenesis scenario [1] is based on the seesaw (type I) mechanism, consisting of the Standard Model (SM) extended by 2 or 3 right-handed (RH) Majorana neutrinos with hierarchical masses. The lightest RH neutrino, produced by thermal scattering after inflation, decays through out-of-equilibrium processes that violate lepton number, C and CP symmetries. These processes induce a dynamical production of a lepton asymmetry, which can be converted into a baryon asymmetry through $(B + L)$ -violating sphaleron interactions. In this context, several studies [2, 3, 5] investigated this possible explanation of the baryon asymmetry of the Universe (BAU) and the different analyses have led to constraints on neutrino physics from the requirement of a successful leptogenesis. For instance, a lower bound on the reheating temperature T_{RH} (see e.g. [3, 4, 6]) and an upper bound on the absolute scale of light neutrino masses (for example in [7]) have been derived. These studies have been performed using the so called “one-flavour state” approximation. It is becoming well known that the explanation of the BAU from a successful thermal leptogenesis has to be revisited when the mass of the decaying right-handed neutrino that produces the lepton asymmetry is $M_{N_1} \lesssim 10^{12}$ GeV [8, 14]. In this case, the Yukawa couplings of the charged leptons affect the dynamics of the Boltzmann equations (BE) and one cannot use the usual one-state-dominance approximation (one flavour), but the “flavoured” dynamical equations in the derivation of the BAU must be taken into account [8]-[14].

2 Flavours in leptogenesis

We consider the SM Lagrangian with three heavy Majorana right-handed neutrinos N_i , $i = 1, 2, 3$. The RH neutrinos couple to the left-handed (LH) ones through the complex Yukawa coupling matrix, λ . The small neutrino masses generated by the seesaw (type I) mechanism are given by :

$$m_\nu = v^2 U^T \lambda^T \mathcal{M}^{-1} \lambda U , \quad (1)$$

where U is the PMNS mixing matrix, v is the vacuum expectation value (vev) of the Higgs field ($v \simeq 174$ GeV), and \mathcal{M} is the 3×3 diagonal Majorana mass matrix. We assume a hierarchical spectrum for the right handed neutrino, $M_{N_3} \gg M_{N_2} \gg M_{N_1}$, and consider that the lepton asymmetry is produced by the decay of the lightest RH neutrino N_1 . Then, in the context of leptogenesis, the baryon asymmetry is obtained by partial conversion of the leptonic asymmetry via sphaleron interactions. With the correct treatment of flavoured leptogenesis, this conversion reads [9] :

$$Y_B \simeq \frac{12}{37} \sum_{\alpha} Y_{\Delta\alpha} . \quad (2)$$

$Y_{\Delta\alpha}$ is the $B/3 - L_\alpha$ asymmetry in the lepton flavour α , which is conserved by sphaleron interactions and transmitted to a baryonic asymmetry Y_B .

Defining the variable $z = M_1/T$, the BE governing the abundance of RH neutrinos Y_{N_1} , and the asymmetry $Y_{\Delta\alpha}$ are [11]:

$$Y'_{N_1}(z) = -\kappa(D(z) + S(z))(Y_{N_1}(z) - Y_{N_1}^{eq}(z)), \quad (3)$$

$$Y'_{\Delta\alpha}(z) = -\epsilon_\alpha\kappa(D(z) + S(z))(Y_{N_1}(z) - Y_{N_1}^{eq}(z)) - \kappa_\alpha W(z) \sum_\beta A'_{\alpha\beta} Y_{\Delta\beta}(z), \quad (4)$$

where $Y_{N_1}^{eq}$ is the thermal population of the lightest RH neutrino N_1

$$Y_{N_1}^{eq}(z) \simeq \frac{45\zeta(3)}{2\pi^4 g_\star} \frac{3}{4} z^2 K_2(z), \quad (5)$$

with $g_\star = 106.75$ in the SM. The CP-asymmetry generated by N_1 in the flavour α is given by [10]:

$$\begin{aligned} \epsilon_\alpha &= \frac{\Gamma_{N_1 \ell_\alpha} - \Gamma_{N_1 \bar{\ell}_\alpha}}{\sum_\alpha (\Gamma_{N_1 \ell_\alpha} + \Gamma_{N_1 \bar{\ell}_\alpha})} \\ &= \frac{1}{(8\pi)} \frac{1}{[\lambda\lambda^\dagger]_{11}} \sum_j \text{Im} \{ (\lambda_{1\alpha})(\lambda\lambda^\dagger)_{1j}(\lambda_{j\alpha}^*) \} g \left(\frac{M_j^2}{M_1^2} \right), \end{aligned} \quad (6)$$

where g is the usual loop function [15].

In eqs. (3,4), the wash-out parameters have been factorized out, and are defined as follows:

$$\kappa_\alpha \equiv \frac{\Gamma_{N_1 \ell_\alpha}}{H(M_{N_1})} = \lambda_{1\alpha} \lambda_{1\alpha}^* \frac{v^2}{M_1 m^*} \equiv \frac{\tilde{m}_\alpha}{m^*}, \quad (7)$$

$$\kappa = \sum_\alpha \kappa_\alpha \equiv \frac{\tilde{m}}{m^*}, \quad (8)$$

with m^* the equilibrium neutrino mass, $m^* \simeq 1.08 \times 10^{-3}$ eV. These parameters exhibit the out-of-equilibrium condition on the decay of the right-handed neutrino: the decay process is out-of-equilibrium when the decay rate is slower than the Hubble expansion rate at the temperature M_{N_1} : $\Gamma \lesssim H(M_{N_1})$ and thus $\kappa \lesssim 1$. The regime where $\kappa \ll 1$ is called the weak wash-out regime, in which case the inverse reactions involving the thermal scatters are rather slow and do not efficiently wash-out the lepton asymmetry. On the contrary, $\kappa \gg 1$ is the strong wash-out regime, where the inverse reactions strongly wash-out the asymmetry. Depending on the value of this wash-out parameter, analytical approximations of the production and wash-out terms allow us to derive semi-analytical formulae for the baryon asymmetry, as will be seen in the next section. The processes we take into account in eqs. (3,4) are decays and inverse decays labeled $D(z)$, and $\Delta L = 1$ scattering, $S(z)$. Notice that in eq. (4), CP violation in scattering is also taken into account, and thus $S(z)$ further contributes to the production of the $Y_{\Delta\alpha}$ asymmetry. In this study we neglect $\Delta L = 2$ scatterings (except the real intermediate states already subtracted) that are negligible as $M_{N_1}/10^{14}$ GeV $\ll 0.1 \times \kappa$ [11], as well as scatterings involving gauge bosons. The thermally averaged decay rate is given by:

$$D(z) = z \frac{K_1(z)}{K_2(z)}, \quad (9)$$

where $K_n(z)$ are the modified Bessel functions of the 2nd kind. The Higgs-mediated scatterings in the s - and t -channel contribute to the production of the asymmetry, as well as to the wash-out term. Their effects can be parametrized by two functions $f_1(z)$ and $f_2(z)$:

$$f_1(z) = \frac{S(z) + D(z)}{D(z)} \simeq \frac{0.1}{z^2} \left(\frac{15}{8} + z \right) \left[1 + a_h(z) z^2 \log \left(1 + \frac{0.1}{a_h(z) z} \right) \right], \quad (10)$$

$$f_2(z) \simeq \frac{0.1}{z^2} \left(\frac{15}{8} + z \right) \left[\mu(\kappa) + a_h(z) z^2 \log \left(1 + \frac{0.1}{a_h(z) z} \right) \right], \quad (11)$$

where $a_h(z) \simeq \log(\frac{M_1}{M_h(T)}) \simeq \log(\frac{z}{0.4})$ and $\mu(\kappa) \simeq 1$ (2/3) in the case of weak (strong) wash-out regime. The wash-out term $W(z)$ contains a part from the inverse decay and a part from scatterings [5] and is given by:

$$W(z) = W_{ID}(z) f_2(z), \quad W_{ID}(z) = \frac{1}{4} z^3 K_1(z). \quad (12)$$

The function $f_1(z)$ ($f_2(z)$) parametrizes the effect of the scatterings in the production (wash-out) factor, and the r.h.s. of eqs.(10,11) comes from high-temperature approximations of the reduced-cross sections, when the scattering effects are fully relevant. In the low temperature regime, scatterings become negligible, so the functions f_1 and f_2 tend to unity. The matrix $A_{\alpha\beta}$ ¹ depends on which charged lepton interactions are in thermal equilibrium, and parametrizes the conversion of the leptonic asymmetry into a $B/3 - L_\alpha$ asymmetry according to $Y_\alpha = \sum_\beta A_{\alpha\beta} Y_{\Delta\beta}$. If the temperature at which leptogenesis occurs, M_1 , is below 10^9 GeV, interactions involving charged μ and τ couplings are fast compared to the Hubble expansion rate, and are therefore in equilibrium. Thus, μ and τ flavours have to be treated separately and so the electron flavour is also distinguishable. Then one has [11]:

$$A = -A' = \begin{pmatrix} -151/179 & 20/179 & 20/179 \\ 25/358 & -344/537 & 14/537 \\ 25/358 & 14/537 & -344/537 \end{pmatrix}. \quad (13)$$

For M_1 between 10^9 GeV and 10^{12} GeV, only the charged τ Yukawa interactions are in equilibrium. The interactions involving the e and μ flavours are slower than the expansion rate, so that those flavours are indistinguishable, and the decay of N_1 will generate a $Y_{e+\mu}$ asymmetry. The ‘‘flavoured’’ asymmetries are then reduced to $(Y_\tau - Y_{e+\mu})$, and the $B - L \leftrightarrow L$ conversion matrix reads :

$$A = -A' = \begin{pmatrix} -417/589 & 120/589 \\ 30/589 & -390/589 \end{pmatrix}. \quad (14)$$

In a recent work [14], it has been argued that the interaction rates involving the charged Yukawa couplings should be fast compared to the interactions involving the decaying N_1 in order to have sufficient time to project the produced lepton asymmetry onto flavour-space. It has been derived that M_{N_1} should be below 5×10^{11} GeV for the tau-Yukawa to be in equilibrium, hence projecting the lepton asymmetry on the $(Y_\tau - Y_{e+\mu})$ space. This point will be discussed in section 4.

A formal solution of eq. (4) for the $B/3 - L_\alpha$ asymmetry is given by:

$$Y_{\Delta\alpha}(z) = -\epsilon_\alpha \kappa \int_{z_{in}}^z dx D(x) f_1(x) \Delta N_1(x) e^{-\kappa_\alpha A'_{\alpha\alpha} \int_x^z dy W(y)} \quad (15)$$

$$- \kappa_\alpha \sum_{\beta \neq \alpha} A'_{\alpha\beta} \int_{z_{in}}^z dx W(x) Y_{\Delta\beta}(x) e^{-\kappa_\alpha A'_{\alpha\alpha} \int_x^z dy W(y)},$$

where $\Delta N_1(z) = (Y_{N_1}(z) - Y_{N_1}^{eq}(z))$ is the departure from thermal equilibrium. The first term in eq. (15) had been estimated for a vanishing initial N_1 abundance, $N_1(z_{in}) = 0$, and for an N_1 abundance initially at thermal equilibrium² $N_1(z_{in}) = N_1(z_{in})^{eq}$, in Refs. [5, 11, 12]. The second term, which has been neglected in these previous studies, is responsible for the interdependency of the flavours through the off-diagonal matrix elements $A'_{\alpha\beta}$. This term drives a new contribution to the $B/3 - L_\alpha$ asymmetry and can be relevant. In some cases the latter is in fact the dominant contribution, as we will later see.

We parametrize, as usual, the final asymmetry $Y_{\Delta\alpha}$ in terms of efficiency factors that contain all the dependency on the wash-out factors κ, κ_α . Those efficiencies η_α are defined by:

$$Y_{\Delta\alpha} \equiv -\epsilon_\alpha \eta_\alpha Y_{N_1}^{eq}(T \gg M_{N_1})$$

$$\simeq -3.9 \times 10^{-3} \epsilon_\alpha (\eta_\alpha^d + \eta_\alpha^{nd}). \quad (16)$$

The first term η_α^d has been derived in [11, 12], and its expression will be presented in the next section. The second term, η_α^{nd} , arises from the non-diagonal conversion of a leptonic flavour, say L_β , into the $B/3 - L_\alpha$ direction and its effect is also studied in the next section. It is clear from eq. (15) that the efficiency η_α of the process depends on the individual wash-out parameter κ_α , but weighted by the factor $A'_{\alpha\alpha}$ arising from the $B - L \leftrightarrow L$ conversion. We then define $\tilde{\kappa}_\alpha \equiv A'_{\alpha\alpha} \kappa_\alpha$ (and consequently $\tilde{\kappa} = \sum_\alpha \tilde{\kappa}_\alpha$) as the ‘‘real’’ wash-out parameter, and thus $\eta_\alpha = \eta(\tilde{\kappa}_\alpha)$.

The baryon asymmetry reads:

$$Y_B = \frac{12}{37} \sum_\alpha Y_{\Delta\alpha} \simeq -1.26 \times 10^{-3} \sum_\alpha \epsilon_\alpha \eta_\alpha, \quad \text{with } \eta_\alpha = \eta_\alpha^d + \eta_\alpha^{nd}. \quad (17)$$

¹For convenience we use $A' = -A$ in the BE so that the diagonal elements are positive.

²We will refer to the case of a vanishing initial abundance as a dynamical case, as the population of N_1 is created dynamically by thermal processes. The case of a N_1 initially at thermal equilibrium will be referred as thermal case, even if it requires a non-thermal production mechanism.

The baryon asymmetry is, as the lepton asymmetry, the sum of the diagonal term proportional to $A_{\alpha\alpha} \simeq 1$ and of the off-diagonal term proportional to $A_{\alpha\beta, \beta \neq \alpha} \simeq 1/10$. The latter contribution will be negligible for the baryon asymmetry, but will strongly modify the individual lepton asymmetries.

3 Efficiency factors

Here we proceed to numerically solve the BE (eqs. (3,4)) for different configurations of the individual CP asymmetries and wash-out factors, for distinct flavour ‘‘alignments’’.

3.1 Study of the efficiency η^d

In this part, we neglect the off-diagonal part in the last term of eq. (4) and solve the BE (eqs. (3,4)). Depending on the initial conditions and on the strenght of the wash-out, several analytical approximations can be derived for η^d (eq. (16)).

3.1.1 Vanishing initial N_1 abundance

In the case where the population of N_1 is dynamically generated, i.e. $N_1(z_{in}) = 0$, one can derive the expression for η^d in different wash-out regimes [11]:

- all flavours in the strong wash-out case: $\kappa_\alpha \gg 1$

$$\eta^d(\tilde{\kappa}_\alpha) \simeq 3.5 \left(\frac{1}{6\tilde{\kappa}_\alpha} \right)^{1.16}, \quad (18)$$

- all flavours in the weak wash-out case: $\kappa_\alpha \ll 1$,

$$\eta^d(\tilde{\kappa}_\alpha) \simeq 1.4 \tilde{\kappa}_\alpha \tilde{\kappa}. \quad (19)$$

However, within the choosen range of wash-out parameter, we find that the efficiency is better fitted with $\eta^d(\tilde{\kappa}_\alpha) \simeq 0.4 \tilde{\kappa}_\alpha \sqrt{\tilde{\kappa}}$, as can be seen in fig.1.

- some flavours in strong $\kappa_\alpha \gg 1$ and some others in weak $\kappa_\beta \ll 1$ wash-out regimes. In this case the efficiency for the flavour α is given by eq. (18) and the efficiency for the flavour β is given by:

$$\eta^d(\tilde{\kappa}_\beta) \simeq 0.3 \tilde{\kappa}_\beta. \quad (20)$$

The efficiency η^d is then obtained by simple interpolation between these three generic cases. For the sake of illustration, we choose 3 representative cases:

- Case a): all the wash-out parameters κ_α are equal.
- Case b): some flavours (e.g. β) are weakly washed-out with $\kappa_\beta = 5 \times 10^{-2}$.
- Case c): some flavours (β) are strongly washed-out with $\kappa_\beta = 30$.

We checked the validity of those expressions in the considered range of wash-out parameters, κ_α between 10^{-2} and 10^2 . It is interesting to notice the dependence of η_α^d on the total wash-out parameter κ in eq. (19). From this term, a flavour α that is weakly washed-out will be sensitive to the wash-out of the other flavours implying that there is a correlation of the flavours. This can be seen in figure 1, where we represent the efficiency of a given flavour (α) as a function of the respective wash-out parameter κ_α , for the three representative cases a), b) and c) discussed above. The democratic scenario, case a), which is similar to the one-flavour approximation, is represented in red and the misaligned cases b) and c) are represented in blue and green, respectively. For comparison, we also represent the analytical estimates (dashed lines) of the efficiencies, eqs. (18-20). We see that the agreement between the numerical and the analytical results is very good.

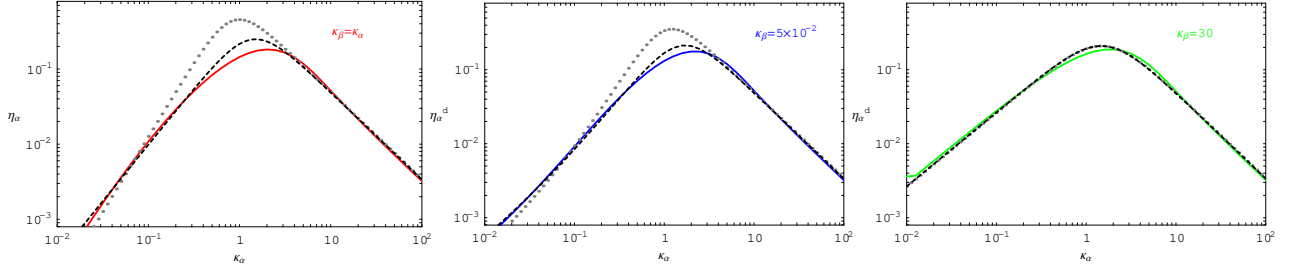


Figure 1: Efficiency $\eta^d(\tilde{\kappa}_\alpha)$ in the dynamical case, for specific values of κ_β , $\beta \neq \alpha$. Case a) (red curves): $\kappa_\beta = \kappa_\alpha$; case b) (blue curves): $\kappa_\beta = 5 \times 10^{-2}$; case c) (green curves): $\kappa_\beta = 30$. In each case, the solid lines represent the numerical computation and the dashed ones the results of the analytical approximation. In the left panel, the upper (dotted) curve corresponds to the analytical estimates of the efficiency in the weak wash-out regime eq. (19).

Firstly, in the case where the right handed neutrino population is created by inverse decays and scatterings, the wash-out factor which parametrizes the strenght of those thermal production, has to be non-negligible in order to produce a sufficient amount of N_1 . Therefore, the efficiency is maximized in this dynamical case for $\kappa_\alpha \simeq 1$ with $\eta_{dyn}^{max} \simeq 0.2$.

Secondly, and this is the main point here, we see that the efficiency of the process when the flavour α is weakly washed-out does indeed depend on the strenght of the wash-out of the other flavours. For example, for $\kappa_\alpha \simeq 5 \times 10^{-2}$ (and assuming $A'_{\alpha\alpha} \simeq A'_{\beta\beta} \simeq 1$), we roughly have $\eta_\alpha^{(b)} \simeq \eta_\alpha^{(c)} \simeq 3 \times 10^{-3}$ and $\eta_\alpha^{(c)} \simeq 1.5 \times 10^{-2}$.

The enhancement $\eta^{(c)}$ comes from the fact that $\kappa \simeq 10$ but still $\kappa_\alpha \lesssim 1$, and the eq.(20) applies. For cases a) and b), eq.(19) applies, and we have an extra supression from the factor $\kappa \simeq 10^{-1}$. Looking at the strong wash-out regime, $\kappa_\alpha > 1$, we see that the efficiency of the flavour α does not depend on the wash-out of the other flavours.

3.1.2 Thermal initial abundance

In the case where the population of N_1 is initially in thermal equilibrium, $N_1(z_{in}) = N_1(z_{in})^{eq}$, the computation of the efficiencies is modified. Following [5, 12], one has for the efficiency factors:

$$\eta^d(\tilde{\kappa}_\alpha) \simeq \frac{2}{\tilde{\kappa}_\alpha z_B(\tilde{\kappa}_\alpha) f_1(z_B(\tilde{\kappa}_\alpha))} \left(1 - e^{-\frac{1}{2} [\tilde{\kappa}_\alpha z_B(\tilde{\kappa}_\alpha) f_1(z_B(\tilde{\kappa}_\alpha))]} \right), \quad (21)$$

where

$$z_B(\tilde{\kappa}) \simeq 2 + 4 \tilde{\kappa}^{0.13} e^{-2.5/\tilde{\kappa}}. \quad (22)$$

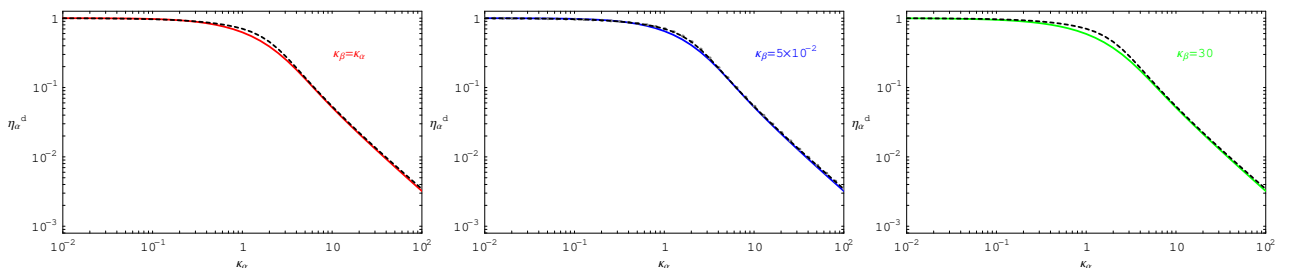


Figure 2: Efficiency $\eta^d(\tilde{\kappa}_\alpha)$ in the case of a thermal initial N_1 abundance, for specific values of κ_β , $\beta \neq \alpha$. Line and color code as in figure 1.

The study of the thermal case is shown in figure 2, where we again consider the 3 cases a), b) and c), with the same colour code as in figure 1. The difference from the case of a vanishing initial N_1 is striking

in the weak wash-out regime: besides the obvious behaviour of η that is maximized for small wash-out, $\eta_{ther.}^{max} \simeq 1$ for $\kappa_\alpha \ll 1$, we see that the effect of flavour is negligible, except for $\kappa_\alpha \simeq 1$, where a small distinction of the cases a), b) and c) is possible. In the strong wash-out regime, the individual efficiencies do not depend on the wash-out of other flavours, as in the dynamical case. Furthermore, in this strong wash-out regime, there is no distinction between the thermal and the dynamical cases, as can be seen in the left panel of figure 4 which is included in the discussion of the next section. We also see that the agreement between the analytical result for the efficiency given in eq. (21) and the numerical result is very good.

3.2 Study of η^{nd}

Now we study the effect of the non-diagonal terms $A_{\alpha\beta}$, $\alpha \neq \beta$, that exhibit the interplay between different flavours. This interplay can be seen in the last term of eq. (15):

$$-Y_{\Delta\alpha}^{nd} = 3.9 \times 10^{-3} \epsilon_\alpha \eta_\alpha^{nd} = \kappa_\alpha \sum_{\beta \neq \alpha} A'_{\alpha\beta} \int_{z_{in}}^z dx W(x) Y_{\Delta\beta}(x) e^{-\kappa_\alpha A'_{\alpha\alpha} \int_x^z dy W(y)}. \quad (23)$$

One can find an approximate expression for this term: considering that the variations of $Y_{\Delta\beta}(x)$ are negligible compared to the rest of the integrand, one can approximate it to its final value $Y_{\Delta\beta}(x) \simeq Y_{\Delta\beta}(\infty)$, and can thus be factorized out from the integral. Another approximation is to consider that $Y_{\Delta\beta}$ is mainly generated by the diagonal part, that is we neglect the effects of $\mathcal{O}(A_{nd}^2)$ that are corrections of the order of a few percent. We obtain:

$$3.9 \times 10^{-3} \epsilon_\alpha \eta_\alpha^{nd} \simeq \kappa_\alpha \sum_{\beta \neq \alpha} A'_{\alpha\beta} Y_{\Delta\beta}^d f_c(\tilde{\kappa}_\alpha), \quad (24)$$

where $\tilde{\kappa}_\alpha = \kappa_\alpha A'_{\alpha\alpha}$ and $f_c(\tilde{\kappa}_\alpha)$ is given by:

$$f_c(\tilde{\kappa}_\alpha) = \int_{z_{in}}^\infty dx W(x) e^{-\tilde{\kappa}_\alpha \int_x^\infty dy W(y)} \quad (25)$$

$$\simeq 1.3 \frac{1}{1 + 0.8 \times \tilde{\kappa}_\alpha^{1.17}}. \quad (26)$$

The total efficiency of a given flavour is the sum of the contribution from the diagonal part of A which, contains slight contamination from the other flavours, and from the non-diagonal part, that will be responsible, as we will see, for a huge modification of the total efficiency, in some cases becoming dominant compared to the diagonal contribution,

$$\eta(\tilde{\kappa}_\alpha) = \eta^d(\tilde{\kappa}_\alpha) + \kappa_\alpha f_c(\tilde{\kappa}_\alpha) \sum_{\beta \neq \alpha} A_{\alpha\beta} \frac{\epsilon_\beta}{\epsilon_\alpha} \eta^d(\tilde{\kappa}_\beta). \quad (27)$$

The effect of the non-diagonal part on the asymmetry $Y_{\Delta\alpha}$ depends on the wash-out and on the CP asymmetries of the different flavours. For example, if we consider the flavour α , the asymmetry produced by the diagonal part proportional to η^d depends on the strenght $\tilde{\kappa}_\alpha$. If $\tilde{\kappa}_\alpha \gg 1$, then $Y_{\Delta\alpha}$ is strongly washed-out and therefore is too small, as can be seen in figure 1: for $\kappa_\alpha \gtrsim 100$ we have $\eta^d(\tilde{\kappa}_\alpha) \lesssim 10^{-3}$. Now consider the non-diagonal part: it depends on the strenght of $\tilde{\kappa}_\beta$. If the wash-out of the flavour β is weak (or even mild), then $\eta^d(\tilde{\kappa}_\beta)$ will be close to its maximal value, and then one has in this case:

$$\eta(\tilde{\kappa}_\alpha) \propto \frac{\epsilon_\beta}{\epsilon_\alpha} \eta_{\beta \max}^d \times (10^{-1} - 10^{-2}),$$

the value of η_{\max} depending on the initial conditions. Typically, this effect can, in favourable situations, drive up the asymmetry $Y_{\Delta\alpha}$ by one or two orders of magnitude as can be seen in the different panels of figure 3. There we represent the efficiency factor of a given asymmetry η_α as a function of the wash-out parameter κ_α , for the different alignments of the flavours. We clearly see that the off-diagonal terms of A modify the efficiency η_α in the strong-wash-out case $\kappa_\alpha \gg 1$. Another consequence of this dependence of η_α^{nd} on the wash-out of the other flavours is illustrated in figure 4. We see that when we neglect the off-diagonal terms there is no distinction in the strong wash-out regime between the dynamical and the thermal case. That is, in the strong wash-out regime, the efficiency is independent of the thermal history of the decaying N_1 . However, when we include the off-diagonal terms, we see that for the case c), the

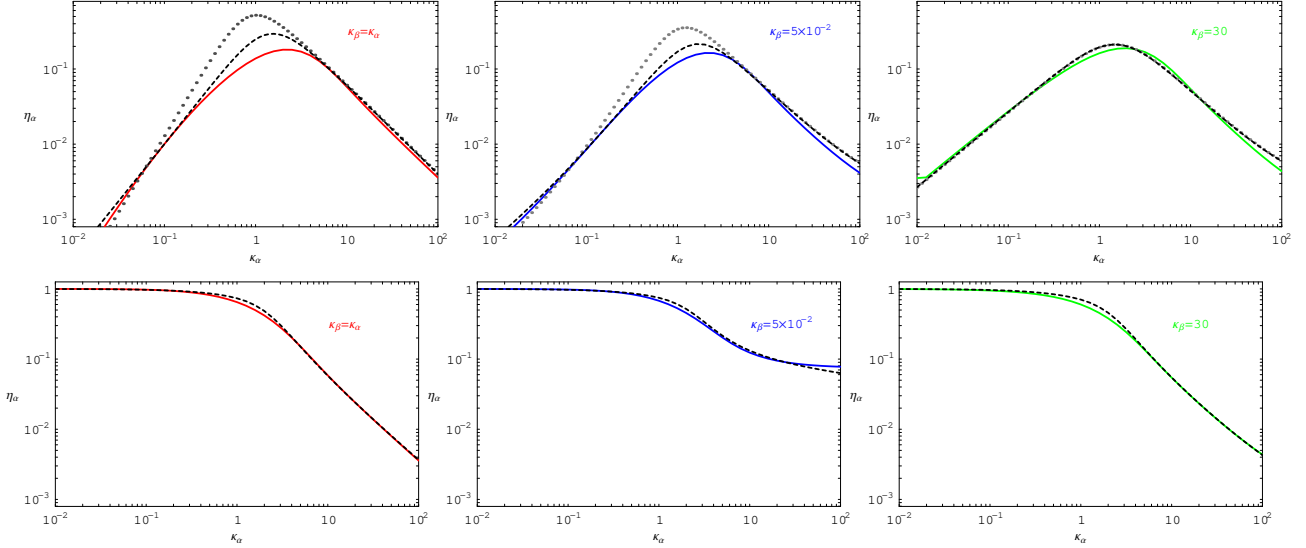


Figure 3:

Influence of the other flavours on the efficiency $\eta(\tilde{\kappa}_\alpha)$. Upper panels: case of a vanishing initial abundance. Lower panels: case of a thermal initial abundance. The curves represent different inputs for the wash-out parameters κ_β , $\beta \neq \alpha$: for the case a) (red curves) we have a democratic scenario where $\kappa_\beta = \kappa_\alpha$, while for the case b) (blue curves) $\kappa_\beta = 5 \times 10^{-2}$ and for the case c) (green curves) $\kappa_\beta = 30$. The solid lines represent the numerical computation and the dashed ones the results of the analytical approximation.

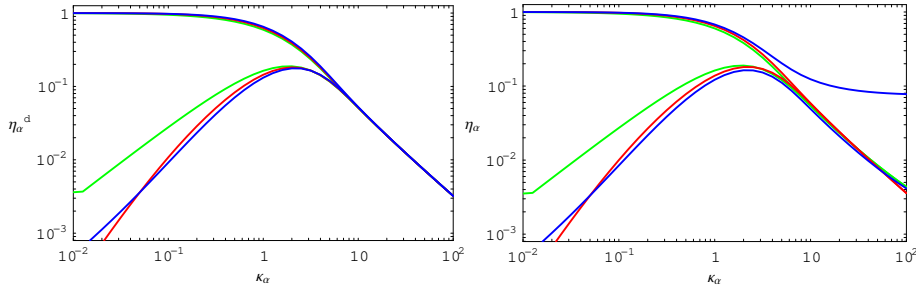


Figure 4:

Influence of the other flavours on the efficiency $\eta(\tilde{\kappa}_\alpha)$. The left panel represents the diagonal contribution to the efficiency, whereas the right panel represents total, the diagonal and non-diagonal contributions. We represent the case of a zero and thermal initial N_1 abundance, for the three cases a), b), c). Line and color code as in figure 1.

two efficiencies do not coincide anymore in the strong wash-out regime, as each $\eta(\tilde{\kappa}_\alpha)$ is related to $\eta^d(\tilde{\kappa}_\beta)$, the latter strongly depending on whether the N_1 was initially at thermal equilibrium or had a vanishing abundance. This clearly illustrates the effect of flavours in leptogenesis.

The above discussion is based on a strong approximation ($Y_{\Delta_\beta}(x) \simeq Y_{\Delta_\beta}(\infty)$), which was made in order to quantify the off-diagonal effect in eq. (23). However this excessively naive approximation does not describe all wash-out and CP asymmetry configurations. Furthermore, the dynamics of the flavours $\beta \neq \alpha$ is neglected and in particular, in the case of a strongly washed-out flavour β , this approximation cannot be used. We thus solve the BE, eqs. (3), (4), including the off-diagonal terms of the A matrix and illustrate in figure 5 contours of the ratio $Y_{e+\mu}/Y_\tau$ (absolute value) in logarithmic scales, for the thermal and dynamical cases, as function of the ratio of the flavoured CP asymmetries $\epsilon_{e+\mu}/\epsilon_\tau$ and of the flavoured wash-out parameters $\kappa_{e+\mu}/\kappa_\tau$. At first sight, we see that $Y_{e+\mu} \geq (\leq) Y_\tau$ for $\epsilon_{e+\mu} \geq (\leq) \epsilon_\tau$.

Looking in more detail, we see that the wash-out parameters influence the former statement. For example, in the thermal case, for $\kappa_{e+\mu}/\kappa_\tau \simeq 0.1$ and $\epsilon_{e+\mu}/\epsilon_\tau \simeq 0.5$, we have $Y_{e+\mu} \sim 2Y_\tau$.

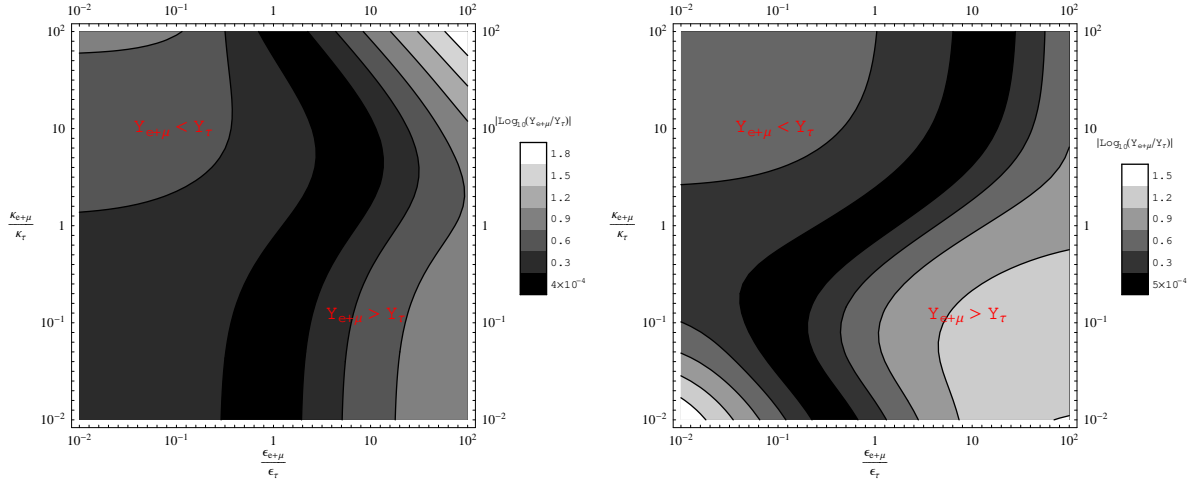


Figure 5: Contour plots of the ratio of the individual flavoured asymmetries, plotted as a function of the ratio of wash-out parameter versus the ratio of CP asymmetries. We place ourselves in a 2 flavour case with $M_{N_1} = 5 \times 10^9$ GeV, $\epsilon_{e+\mu} + \epsilon_\tau = 10^{-6}$ and $\kappa_{e+\mu} + \kappa_\tau = 10$. The left (right) panel stands for the dynamical (thermal) case. On both graphs, the black area denotes the equality $Y_{e+\mu} = Y_\tau$. Moving to the left of this contour, $Y_{e+\mu} < Y_\tau$ whereas to the right we have $Y_{e+\mu} > Y_\tau$.

3.3 The baryon asymmetry

Summing-up the contribution from the diagonal and off-diagonal parts of the A matrix, we finally obtain the baryon asymmetry:

$$Y_B = \frac{12}{37} \sum_{\alpha} Y_{\Delta\alpha} \simeq -1.26 \times 10^{-3} \sum_{\alpha} \epsilon_{\alpha} \eta_{\alpha}. \quad (28)$$

For $\epsilon \equiv \sum_{\alpha} \epsilon_{\alpha} \neq 0$, one can define an efficiency for the baryon asymmetry η_B such that:

$$Y_B = -1.26 \times 10^{-3} \epsilon \eta_B. \quad (29)$$

The baryon asymmetry will be the sum of the individual lepton asymmetries. Therefore, the baryon asymmetry, and hence the efficiency η_B , will depend on the alignment of the flavours. We illustrate this point in figure 6, where the efficiency η_B is plotted as a function of the wash-out parameter κ_{α} , for cases a), b) and c). The solid lines represent the diagonal contributions, and the dashed ones represent both diagonal and non-diagonal contributions. As the baryonic efficiency can be defined only for $\epsilon \neq 0$ and is strongly dependent on the flavoured CP violation ϵ_{α} , we set $\epsilon_{\alpha} = 8 \times 10^{-7}$ for all flavours. First, we

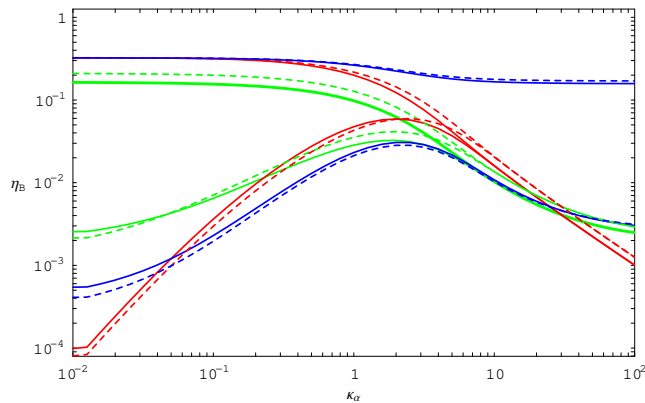


Figure 6: Effects of the off-diagonal terms of the A matrix on the total baryon efficiency η_B .

consider only the diagonal contributions. As expected, we see that the efficiency strongly depends on the

flavour alignment. The democratic scenario (case a), in red) shows the one-flavour approximation-like behaviour. The flavours play a full role in the misaligned case, and especially in case b) (in blue), where we have $\kappa_\beta = 5 \times 10^{-2}$. Then the efficiency for the flavour(s) β is (are) close to its (their) maximum, depending on the thermal history of N_1 . If the flavour α is strongly washed-out, the baryon asymmetry is mainly composed of the flavour(s) β , and is thus weakly washed-out, even if the total wash-out is strong. This is the very effect of taking into account the flavours in leptogenesis. We also see that the baryonic efficiency, as well as the leptonic one, depend on the initial abundance of N_1 in the strong wash-out regime. Now, let us consider the dashed lines, which represent the sum of the diagonal and off-diagonal terms of A . We see that the off-diagonal terms account for percent corrections. A more detailed analysis of their effect on Y_B is shown in fig.7, where we represent contours of $Y_B^{\text{total}}/Y_B^{\text{diagonal}}$ in the interesting two flavour-case. We choose the individual CP asymmetries to be equal, $\epsilon_{e+\mu} = \epsilon_\tau (= 10^{-6})$ but the actual value is not relevant). We see that the off-diagonal terms affect the baryon asymmetry up to 40% in the dynamical case in both ways (increasing and decreasing). On the other hand, the thermal case is only enhanced, up to the same amount. Effects of the off-diagonal terms are particularly important in the strong wash-out regime. In some particular cases the non-diagonal terms also have a relevant role, namely in the democratic

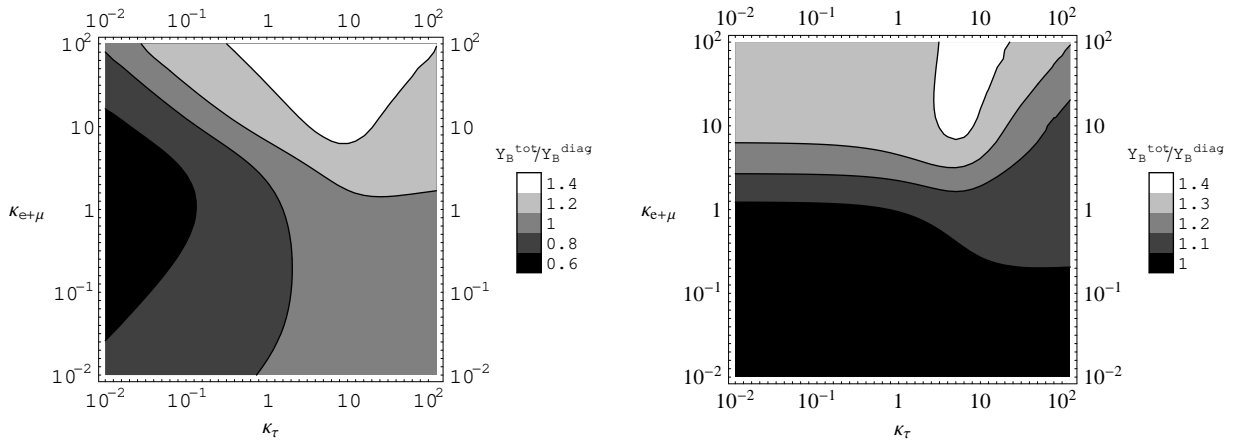


Figure 7:

Effects of the off-diagonal terms on the baryon asymmetry: contour plot of $Y_B^{\text{total}}/Y_B^{\text{diag}}$ for fixed CP asymmetries $\epsilon_{e+\mu} = \epsilon_\tau$ and varying wash-out parameters. The left (right) panel stands for the case of a vanishing (thermal) initial N_1 abundance.

scenario, where $\tilde{\kappa}_\alpha$ are equal, and where the total CP asymmetry is zero $\sum_\alpha \epsilon_\alpha = 0$. Then ignoring the $\mathcal{O}(A)$ effect will lead to a vanishing baryonic asymmetry, as $\sum_\alpha \epsilon_\alpha \eta_{\tilde{\kappa}_\alpha}^d = 0$ [17]. On the contrary, taking into account those effects avoids the latter cancellation. For example, in the case of three distinguishable flavours with the specific alignment in which $\tilde{\kappa}_\alpha = \tilde{\kappa}_\beta = \tilde{\kappa}_\delta$ and $\epsilon_\alpha + \epsilon_\beta + \epsilon_\delta \equiv \epsilon_\alpha(1 + b + d) = 0$, one finds for the baryon asymmetry :

$$Y_B = -1.26 \times 10^{-3} \epsilon_\alpha \eta^d(\tilde{\kappa}_\alpha) \left(\sum_{\alpha_1 \neq \alpha} \kappa_{\alpha_1} f_c(\tilde{\kappa}_{\alpha_1}) A_{\alpha_1 \alpha} + b \sum_{\beta_1 \neq \beta} \kappa_{\beta_1} f_c(\tilde{\kappa}_{\beta_1}) A_{\beta_1 \beta} + d \sum_{\delta_1 \neq \delta} \kappa_{\delta_1} f_c(\tilde{\kappa}_{\delta_1}) A_{\delta_1 \delta} \right).$$

In order to maximize the above function, we take $\alpha = \mu$, $\beta = e$ and $\delta = \tau$ for a positive value of b (in the case of a negative value of b , $\alpha = \mu$, $\beta = \tau$ and $\delta = e$). We then get $Y_B \simeq \epsilon_\mu \eta^d(\tilde{\kappa}_\mu) f_c(\tilde{\kappa}_\mu) \kappa_\mu \times 4.5 \times 10^{-5} (1 + 2b)$, which is non-zero for $b \neq -1/2$.

4 Lower bound on M_{N_1}

When the flavours are taken into account in leptogenesis, the modification of the asymmetry, combined with the change in the efficiency factor may have an impact on the lower bound of the mass of N_1 . From

the bound on each individual CP asymmetry [10],

$$\epsilon_\alpha \lesssim \frac{3M_{N_1}m_{\max}}{16\pi v^2} \sqrt{\frac{\kappa_\alpha}{\kappa}}, \quad (30)$$

one has

$$\begin{aligned} |Y_B| &\simeq 1.26 \times 10^{-3} \sum_\alpha \epsilon_\alpha \eta_\alpha \\ &\lesssim 1.26 \times 10^{-3} \frac{3M_{N_1}m_{\max}}{16\pi v^2} \sum_\alpha \sqrt{\frac{\kappa_\alpha}{\kappa}} \eta_\alpha, \end{aligned} \quad (31)$$

from which a lower bound on M_{N_1} is derived,

$$M_{N_1} \gtrsim \frac{16\pi}{3 \times 1.26 \times 10^{-3}} \frac{v^2}{m_{\max}} \frac{|Y_B|}{\sum_\alpha \sqrt{\frac{\kappa_\alpha}{\kappa}} \eta_\alpha} \quad (32)$$

$$M_{N_1} \gtrsim 7.1 \times 10^8 \text{ GeV} \left(\frac{m_{\text{atm}}}{m_{\max}} \right) \left| \frac{Y_B}{Y_B^{CMB}} \right| \frac{1}{\sum_\alpha \sqrt{\frac{\kappa_\alpha}{\kappa}} \eta_\alpha}. \quad (33)$$

Since the lower bound on M_{N_1} is inversely proportional to the efficiency η_α , it will therefore depend on the thermal history of the decaying right-handed neutrino. In the case where N_1 are produced by scatterings, the efficiency is maximized for a wash-out $\kappa_\alpha \simeq 1$, where $\eta_\alpha \simeq 0.2$. In the case where N_1 are non-thermally produced, the efficiency is maximized to 1 for a very weak wash-out $\kappa_\alpha \ll 1$. The lower bound will depend on the alignment of flavours, and in the democratic case one has:

$$M_{N_1} \gtrsim \begin{cases} 4.1 \times 10^8 \text{ GeV} & \text{in the thermal case} \\ 2.5 \times 10^9 \text{ GeV} & \text{in the dynamical case.} \end{cases} \quad (34)$$

This bound is close to the one derived in the ‘‘one flavour approximation’’, where $M_{N_1} \gtrsim 2.1 \times 10^8 \text{ GeV}$ in the thermal case and $M_{N_1} \gtrsim 1.05 \times 10^9 \text{ GeV}$ in the dynamical one [7]. Besides flavour effects, the difference between the lower bounds of the flavoured and unflavoured cases comes from a different factor in the $B - L \leftrightarrow B$ conversion. Indeed, in the one flavour dominance, the Davidson-Ibarra bound reads [6]:

$$\epsilon \leq \frac{3}{8\pi} \frac{M_{N_1}m_{\max}}{v^2}, \quad (35)$$

and the conversion from sphalerons is $Y_B = 28/51Y_L$. Therefore the lower bound on M_{N_1} in the unflavoured case is $\sim 1/2 \times 12/37 \times 51/28 \sim 0.3$ times the flavoured one.

An implication of this bound resides in the well-known conflict between the reheating temperature and leptogenesis. Indeed, T_{RH} should be above M_{N_1} in order to avoid the erasing of the lepton asymmetry. In view of the above estimates, $T_{RH} \gtrsim 4 \times 10^{9(8)} \text{ GeV}$ in the dynamical (thermal) case. In this case, the inclusion of flavours does not really help. In the regime of strong wash-out, $\kappa \gg 1$, where the effective neutrino mass is close to the mass inferred from atmospheric oscillations, the situation changes. In the one-flavour approximation, the efficiency $\eta(\kappa) \propto \kappa^{-1}$, therefore $M_{N_1}^{\text{min}} \propto \kappa$, and increases with the wash-out, and so does the reheating temperature. In this strong wash-out regime, we roughly estimate $T_{RH} \geq M_{N_1}/10 \simeq 9 \times 10^8 \text{ GeV} \kappa$, $\kappa \gg 1$ [5]. Including flavours, one generically has non-alignment of the individual asymmetries, and one can have a strong total wash-out, with some weakly washed-out flavours. If for example (see fig. 8), $\kappa \simeq m_{\text{atm}}/m^* \simeq 45$ with $\kappa_\beta \simeq 40$ but $\kappa_\alpha \simeq 5$, one has $M_{N_1}^{\text{min}} \simeq 2 \times 10^{10} \text{ GeV}$ for the flavoured case and $8 \times 10^{10} \text{ GeV}$ for the unflavoured case. Hence, including flavours, the reheating temperature in this strong wash-out regime is lowered by a factor $\simeq 4$, and one roughly has $T_{RH} \geq 2 \times 10^9 \text{ GeV}$.

4.1 Numerical results

We numerically solve the set of coupled BE (eqs.(34)) and obtain the allowed parameter space. The input parameters of the BE are the Yukawa couplings λ , which define the wash-out parameters and the CP asymmetries. These have been built using the Casas-Ibarra parametrization [16]. In this parametrization the matrix λ reads:

$$\lambda = M_N^{1/2} R m^{1/2} U^\dagger v^{-1}, \quad (36)$$

U being the PMNS matrix parametrized by three angles and three phases. The solar and atmospheric angles are well measured, whereas the θ_{13} angle (Chooz angle) is only upper-constrained. The three CP violating phases are yet undetermined. The matrix R is a 3×3 orthogonal matrix depending on three complex angles. We impose a normal hierarchical spectrum, both for the light and for the heavy neutrino sectors, so that the only free parameters that enter in the mass matrix are the lightest neutrino masses m_1 and M_{N_1} . Therefore, we have 12 independent variables that are not experimentally determined.

In our numerical computation, we scan over the whole parameter space by randomly choosing the free parameters. Moreover, we impose a perturbative limit $\lambda_{33} \lesssim y_t$ (y_t being the top Yukawa coupling) that will upper-constrain M_{N_1} , leading to the upper bound $M_{N_1} \lesssim 4 \times 10^{11}$ GeV. From [14] and in order for the flavour to be relevant in leptogenesis, an upper bound on M_{N_1} can be derived, namely $M_{N_1} \lesssim 5.8 \times 10^{11}$ GeV. Here, we only consider cases where the interactions involving the charged lepton Yukawas are faster than the inverse decay, so that flavours are fully relevant. Finally, by imposing the obtained baryon asymmetry to be in the experimental range ³, $5.2 \times 10^{-10} \lesssim 7.04 \times Y_B \lesssim 7.2 \times 10^{-10}$, we represent in figure 8 the $(M_{N_1} - \tilde{m})$ parameter space allowed by the requirement of a successful leptogenesis. Many remarks are in order. Firstly, the lower bound numerically derived confirms the one given in eq. (34),

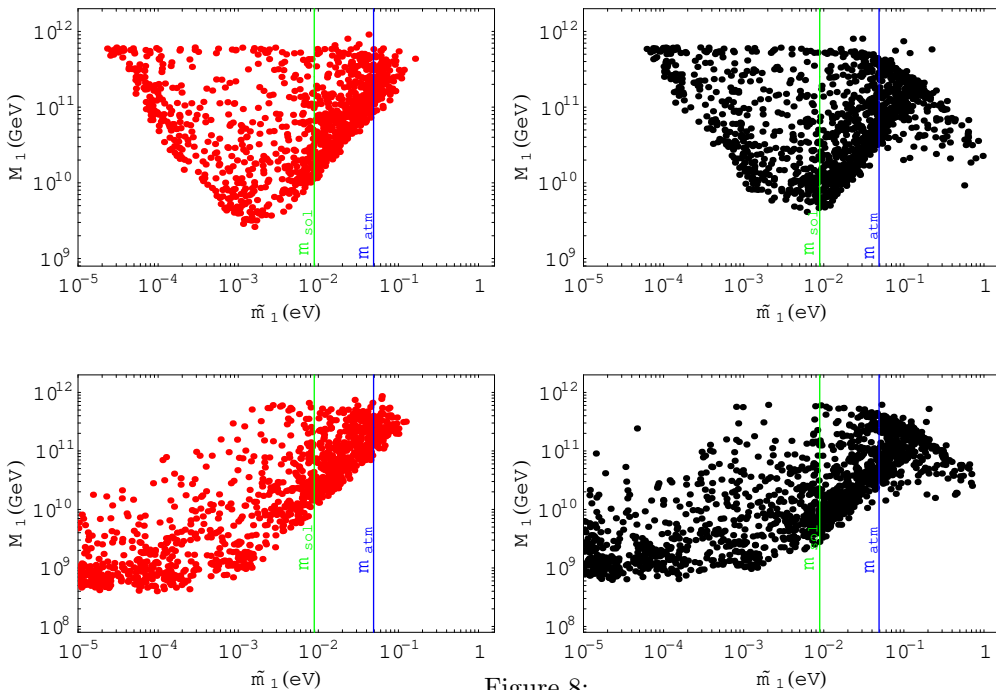


Figure 8:

Successful leptogenesis: bound on M_1 , in the case of a zero (thermal) initial N_1 abundance for the up (down) panels. The left panels show the allowed $(M_{N_1} - \tilde{m})$ parameter space for the one-flavour approximation, whereas the right panels stand for the case when lepton flavours are taken into account. The vertical lines represent $\sqrt{\Delta m_{\text{atm}}^2}$ (in blue) and $\sqrt{\Delta m_{\text{sol}}^2}$ (in green).

and we notice that the “one flavour approximation” (left panels in figure 8) lowers the bound compared to the correct flavour treatment (right panels). Secondly, comparing the dynamical and thermal cases, that is the up and down panels in figure 8, we see that \tilde{m} can take much smaller values in the case of a thermal initial abundance. As this mass encodes the out-of-equilibrium condition, cf. eq. (7), this means that in the thermal case, leptogenesis occurs even for extremely small values of \tilde{m} , while in the dynamical case, this is not possible. Finally, comparing the left and right panels, one clearly sees the effect of flavour in the “re-opening” of the parameter space for higher values of \tilde{m} . Indeed, by introducing the lepton flavour asymmetries, we relax the one-flavour approximation that corresponds either to a common behaviour of the individual asymmetries, or to the dominance of one flavour. Now, other configurations are allowed, and the misaligned ones widen the parameter space. The mass \tilde{m} is related to the total wash-out, that is, to the sum of each individual wash-out. In the one-flavour approximation, a high value of \tilde{m} corresponds to a strong wash-out and is disfavored by leptogenesis. On the contrary we observe (cf. figure 6) that even

³The experimental bounds come from cosmological constraints: the lower bound corresponds to the Big-Bang nucleosynthesis (BBN) constraint on the light species abundance, and the upper-bound from cosmic background radiation (CBR) constraints [18]. The WMAP [19] constraints are included therein.

if the total wash-out is strong, we can still have flavours that are weakly washed-out, hence dominating the baryon asymmetry and allowing a successful leptogenesis. Thus, by the inclusion of flavour in leptogenesis no upper-bound on \tilde{m} can be derived.

Notice that for $\tilde{m}(m_1) \gtrsim \text{atm}$ in figure 8(9), the points drop below the upper-bound $M_{N_1} \simeq 5 \times 10^{11}$ GeV. Indeed, as $m_1 \gtrsim \text{atm}$, $m_{max} \simeq m_1 \simeq m_2 \simeq m_3$, and the upper-bound on M_{N_1} scales as $1/m_1$, c.f eq. (32). In the one flavour approximation, a bound on the light neutrino mass was derived in [7], and this no longer holds when flavours are accounted for [10]. However, in [13] a bound on the neutrino mass scale of about 2 eV is derived in the flavoured leptogenesis context in the strong wash-out regime and hierarchical wash-out factors $1 \ll \kappa_\alpha \ll \kappa_\beta$ and equal CP-asymmetries. In this work, we impose m_ν to be lighter than the cosmological bound $\sum m_\nu \lesssim 1$ eV and we do not explore configurations leading to higher m_ν . This can be seen in figure 9, which represents the allowed parameter space (M_{N_1} - m_1) in different cases. The black points are the result when flavours are included, whereas red ones represent the one-flavour approximation. We clearly see that the cosmological bound is saturated when flavours are considered, and this does not occur in the one-flavour approximation. In figure 9, for m_1 above m_{atm} , the solutions have in general a specific flavour alignment: the flavoured CP-asymmetries are almost equal $\epsilon_{e+\mu} \sim \epsilon_\tau$ and the individual wash-out factors are hierarchical $1 \ll \kappa_\alpha \lesssim 10\kappa_\beta$ and the total wash-out is strong. It is well known that such configurations of wash-out parameters achieve successful leptogenesis in the flavoured case whereas the unflavoured one fails. For such specific configurations, effect of the off-diagonal terms of the A -matrix on Y_B is maximal (c.f fig 7) but nevertheless is only a correction without important impact.

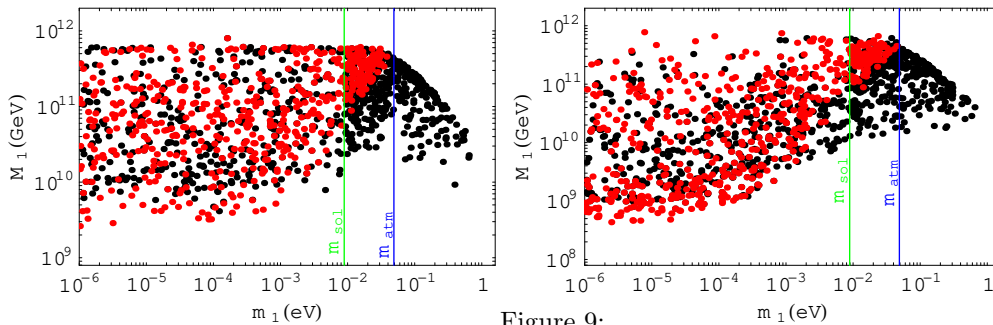


Figure 9:

Successful leptogenesis: M_1 - m_1 space, in the dynamical case (left panel) and in the thermal case (right panel). The vertical lines represent $\sqrt{\Delta m_{\text{atm}}^2}$ (in blue) and $\sqrt{\Delta m_{\text{sol}}^2}$ (in green).

5 Conclusion

The behaviour of individual lepton asymmetries in the case of vanishing initial N_1 abundance has been analysed in [11]. In this study we give semi-analytical results including fine-tuning corrections that depend on flavour alignment. We extend the study to the case of N_1 initially in thermal equilibrium, and confirm that in this case, when off-diagonal entries of the conversion $B/3 - L_\alpha \leftrightarrow L$ are neglected, the efficiency factor for a given flavour is independent of the wash-out of other flavours.

Independently of the thermal history of the decaying right-handed neutrino, we observed that misalignment of flavours can greatly enhance the baryon asymmetry, when compared to the one-flavour approximation, for an identical wash-out strength. We also include off-diagonal entries of the $B/3 - L_\alpha \leftrightarrow L$ conversion that couple flavours among themselves. Even if this inclusion only modifies the baryon asymmetry by a few percent, thus allowing to safely disregard these terms for Y_B computation, we nevertheless stressed that the individual lepton asymmetries are very sensitive to such interdependencies. Finally, we studied the lower bound on the N_1 mass and the leptogenesis allowed parameter space. We confirm the lower bound to be $\sim 4 \times 10^{8(9)}$ GeV for a thermal (vanishing) initial N_1 abundance. We have also shown that the parameter space is enlarged, as the flavour (mis)alignment allows for higher values of the wash-out (or equivalently of \tilde{m}).

Acknowledgements

The authors wish to thank S. Davidson for enlightening discussions and A.M. Teixeira for useful comments and for reading the manuscript. This project is partly supported by the ANR project NEUPAC.

References

- [1] M. Fukugita and T. Yanagida, Phys. Lett. B **174** (1986) 45.
- [2] A partial list: M. A. Luty, Phys. Rev. D **45** (1992) 455; A. Pilaftsis, Phys. Rev. D **56** (1997) 5431 [arXiv:hep-ph/9707235]; W. Buchmuller, P. Di Bari and M. Plumacher, Nucl. Phys. B **643** (2002) 367 [arXiv:hep-ph/0205349]; J. R. Ellis, M. Raidal and T. Yanagida, Phys. Lett. B **546** (2002) 228 [arXiv:hep-ph/0206300]; R. N. Mohapatra and S. Nasri, Phys. Rev. D **71** (2005) 033001 [arXiv:hep-ph/0410369]; Phys. Lett. B **552** (2003) 177 [arXiv:hep-ph/0210271]; G. C. Branco, R. Gonzalez Felipe, F. R. Joaquim, I. Masina, M. N. Rebelo and C. A. Savoy, Phys. Rev. D **67** (2003) 073025 [arXiv:hep-ph/0211001].
- [3] G. F. Giudice, A. Notari, M. Raidal, A. Riotto and A. Strumia, Nucl. Phys. B **685** (2004) 89 [arXiv:hep-ph/0310123].
- [4] S. Antusch and A. M. Teixeira, JCAP **0702** (2007) 024 [arXiv:hep-ph/0611232].
- [5] W. Buchmuller, P. Di Bari and M. Plumacher, Annals Phys. **315** (2005) 305 [arXiv:hep-ph/0401240].
- [6] S. Davidson and A. Ibarra, Phys. Lett. B **535** (2002) 25.
- [7] W. Buchmuller, P. Di Bari and M. Plumacher, Nucl. Phys. B **643** (2002) 367 [arXiv:hep-ph/0205349]; W. Buchmuller, P. Di Bari and M. Plumacher, Phys. Lett. B **547** (2002) 128 [arXiv:hep-ph/0209301]; T. Hambye, Y. Lin, A. Notari, M. Papucci and A. Strumia, Nucl. Phys. B **695** (2004) 169 [arXiv:hep-ph/0312203].
- [8] R. Barbieri, P. Creminelli, A. Strumia and N. Tetradis, Nucl. Phys. B **575** (2000) 61 [arXiv:hep-ph/9911315]; A. Pilaftsis and T. E. J. Underwood, Nucl. Phys. B **692** (2004) 303 [arXiv:hep-ph/0309342]; T. Endoh, T. Morozumi and Z. h. Xiong, Prog. Theor. Phys. **111** (2004) 123 [arXiv:hep-ph/0308276]; O. Vives, Phys. Rev. D **73** (2006) 073006 [arXiv:hep-ph/0512160].
- [9] E. Nardi, Y. Nir, E. Roulet and J. Racker, JHEP **0601** (2006) 164 [arXiv:hep-ph/0601084]; G. Engelhard, Y. Grossman, E. Nardi and Y. Nir, arXiv:hep-ph/0612187; E. Nardi, AIP Conf. Proc. **917** (2007) 82 [arXiv:hep-ph/0702033]; Y. Nir, arXiv:hep-ph/0702199.
- [10] A. Abada, S. Davidson, F. X. Josse-Michaux, M. Losada and A. Riotto, JCAP **0604**, (2006) 004 [arXiv:hep-ph/0601083].
- [11] A. Abada, S. Davidson, A. Ibarra, F. X. Josse-Michaux, M. Losada and A. Riotto, JHEP **0609** (2006) 010 [arXiv:hep-ph/0605281].
- [12] S. Blanchet and P. Di Bari, JCAP **0703** (2007) 018 [arXiv:hep-ph/0607330]; S. Blanchet and P. Di Bari, Nucl. Phys. Proc. Suppl. **168** (2007) 372 [arXiv:hep-ph/0702089].
- [13] A. De Simone and A. Riotto, JCAP **0702** (2007) 005 [arXiv:hep-ph/0611357].
- [14] S. Blanchet, P. Di Bari and G. G. Raffelt, JCAP **0703** (2007) 012 [arXiv:hep-ph/0611337].
- [15] L. Covi, E. Roulet and F. Vissani, Phys. Lett. B **384** (1996) 169 [arXiv:hep-ph/9605319].
- [16] J. A. Casas and A. Ibarra, Nucl. Phys. B **618** (2001) 171 [arXiv:hep-ph/0103065].
- [17] S. Pascoli, S. T. Petcov and A. Riotto, Nucl. Phys. B **774** (2007) 1 [arXiv:hep-ph/0611338].
- [18] G. Steigman, AIP Conf. Proc. **903** (2007) 40 [arXiv:hep-ph/0611209].
- [19] D. N. Spergel *et al.* [WMAP Collaboration], arXiv:astro-ph/0603449.